

# Analysis and Testing of Piles for Ship Impact Defenses

Armin Patsch<sup>1</sup>; Carlos F. Gerbaudo<sup>2</sup>; and Carlos A. Prato<sup>3</sup>

**Abstract:** This paper deals with analyses and reduced scale tests carried out to validate the design of flexible protection structures for bridge piers against ship impact. The protection system analyzed is part of the fixed link currently under construction across the Parana River between the cities of Rosario and Victoria in Argentina, and it will protect a cable-stayed bridge and parts of the approach viaduct against impact of aberrant vessels with sizes up to 100,000 DWT. The protection system was designed on the basis of dissipated energy and consists of groups of steel-encased large diameter concrete piles connected at the top by a reinforced concrete platform. The impact energy is to be absorbed by large horizontal displacements of the pile caps that involve large deformations of the surrounding soil and geometrically and material nonlinear response of the pile shafts themselves. The paper focuses on modeling the nonlinear characteristics of the response of the structure, and on its assessment by means of 1:15 scale model tests performed in both the laboratory and in the field to account for the displacements and deformations undergone by the pile shafts.

**DOI:** 10.1061/(ASCE)1084-0702(2002)7:4(1)

**CE Database keywords:** Ship motion; Piles; Bridges, piers; Impact forces.

## Introduction

### General

The analyses and tests described in this paper were carried out as part of the design and evaluation of the protection system against ship impact of the main components of the fixed roadway connection between the cities of Rosario and Victoria across a heavily navigated stretch of the Paraná River.

With the navigation channel located in the center of the main span of the cable stayed bridge, the pylons and anchor piers of the main bridge, as well as several piers of the access viaduct, are under the risk of impact from ships sailing off this channel by aberration. A detailed presentation of the design concept for the protection system is discussed by the designer (Saul et al. 2001); this paper focuses on the analysis and tests performed by the designer and the independent reviewer to validate the design and the assumptions concerning the mechanical behavior of the soil-pile system.

A general layout of the project is given in Fig. 1, showing the location of the various individual protection structures.

A fleet of bulk carriers, freighters, tankers, barges, and barge-tow configurations sail this waterway. The national authority responsible for the project had set the requirements and standards

for the defense structures to be designed by all participants of the international tender called under a Build-Operate-Transfer general framework. The AASHTO (1991) Guide Specifications for vessel collision design of highway bridges were adopted as a design requirement considering the bridge as a critical structure, together with the application of "Method II" of the guide and impact forces according to Terndrup Pedersen et al. (1993).

The structural analysis and design of the protection structures is the final step in a series of studies and investigations dealing with the impact scenario. These are the ship traffic study, investigation of relevant ship geometry, the geotechnical report, analysis of the natural protection to the configuration of the navigation channel, and analysis of scour at the bridge and in the navigational areas around the bridge. The relevant traffic data from the traffic study and all possible sailing courses were considered and applied in a probabilistic analysis, which is not discussed in this paper. Based on the virtual resistance of piers and/or protection structures, the probabilistic analysis performed by the designer led to the total annual frequency of collapse and to define the design ships and corresponding kinetic energy to be considered for each pier. In the structural design, these design ships were applied sailing on impacting courses perpendicular to the bridge axis.

Verifying that the annual frequency of collapse of  $10^{-4}$  required by the AASHTO Guide is fulfilled requires implementation of not only the protection structures discussed in this paper, but also a number of structural verifications of the superstructure and piers of the main bridge and the access viaducts not addressed here.

To give an idea of the size of these ships and their energy, the design of the defense structures for the main towers was carried out for a design ship of 43,000 displacement tons sailing downstream at 4.64 m/s with a kinetic energy of  $KE = 453$  MNm. The size of this ship is about  $204 \times 32$  m (length  $\times$  width). The amount of energy now considered is more than ten times higher than that adopted 20 years ago for design of the floating defense structures of the Zárrate-Brazo Largo Bridges, located 200 km downstream of the new project (Saul and Svensson 1982, 1983).

<sup>1</sup>Project Engineer, Leonhardt, Andrä und Partner GmbH, D-70192 Stuttgart, Lenzhalde 16, Germany.

<sup>2</sup>Senior Engineer, SETEC SRL, Achával Rodríguez 35, 5000 Córdoba, Argentina.

<sup>3</sup>Professor, National Univ. of Córdoba, Ciudad Universitaria, Córdoba, Argentina.

Note. Discussion open until December 1, 2002. Separate discussions must be submitted for individual papers. To extend the closing date by one month, a written request must be filed with the ASCE Managing Editor. The manuscript for this paper was submitted for review and possible publication on April 25, 2001; approved on August 14, 2001. This paper is part of the *Journal of Bridge Engineering*, Vol. 7, No. 4, July 1, 2002. ©ASCE, ISSN 1084-0702/2002/4-1-9/\$8.00+\$5.00 per page.

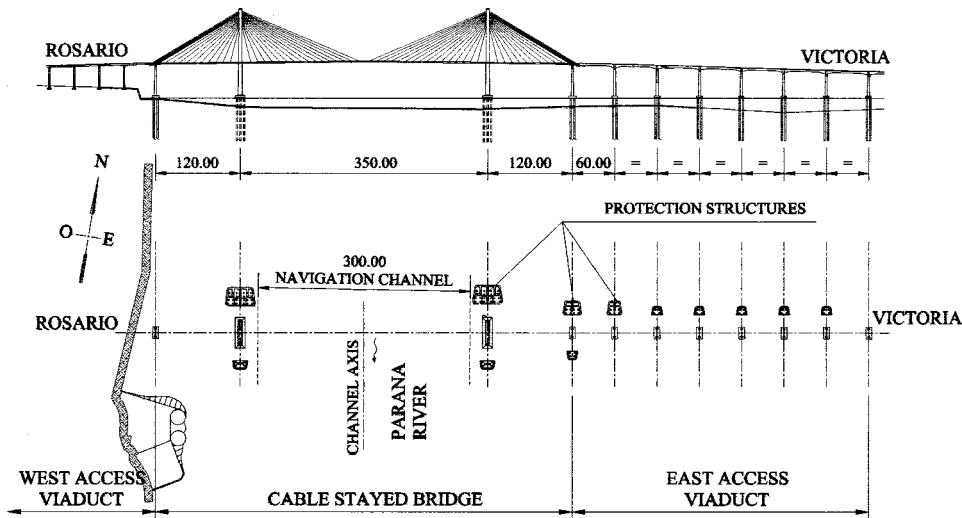


Fig. 1. General layout of protection structures

**Protection Structures**

The selection of the protection system was conditioned by the need to absorb high impact energies and also to cope with erosion and scour in the range of 20–30 m. The pile foundations of the bridge structure itself consist of bored concrete piles 2 m in diameter and approximately 60 m in length. The protection system

adopted consists of a concrete platform supported by sacrificial steel composite piles also 2 m in diameter that undergo large displacements to absorb the impact energy. The elevation of the bottom face of the concrete platform is that of the mean high water level, and an edge beam extends ~2 m below the platform to avoid direct contact of potentially colliding barges with the

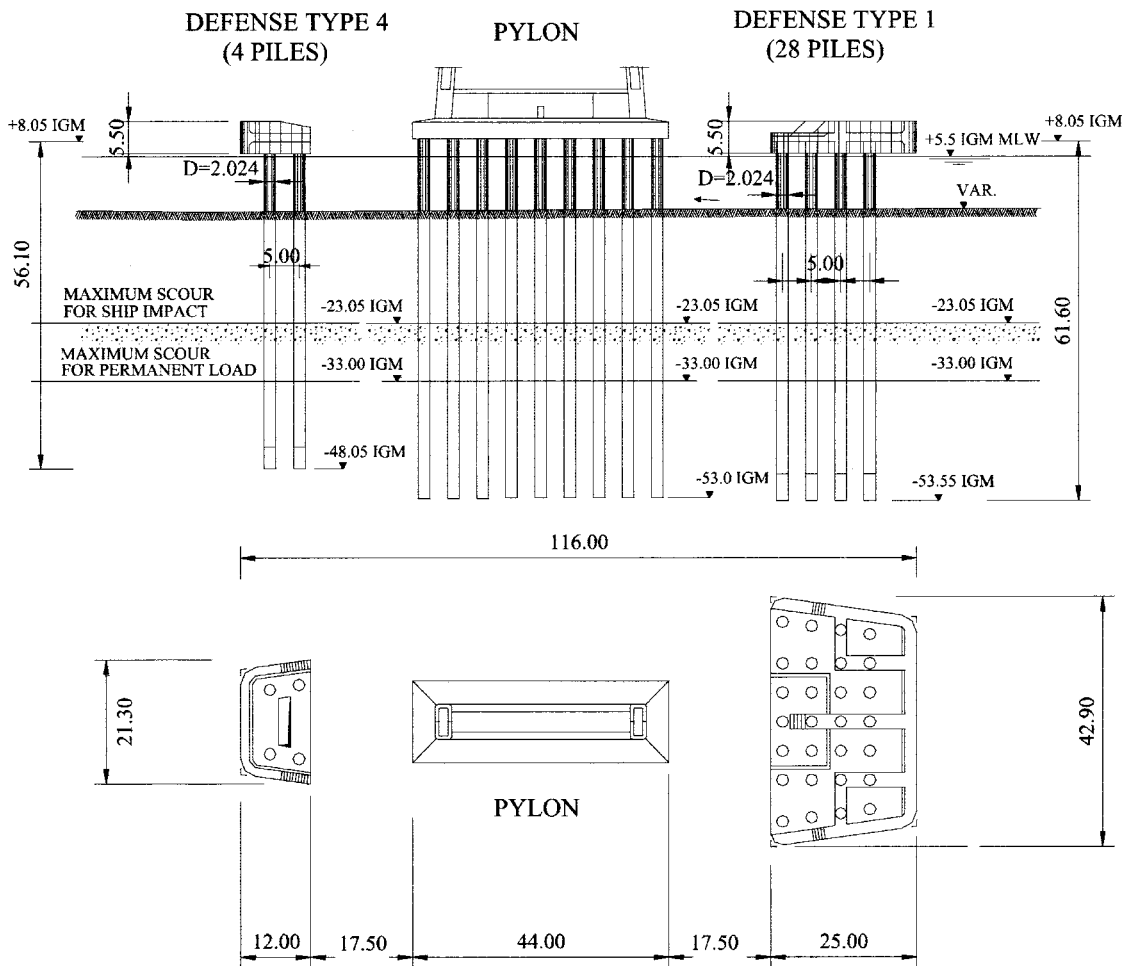


Fig. 2. Protection structure for pylons of main bridge

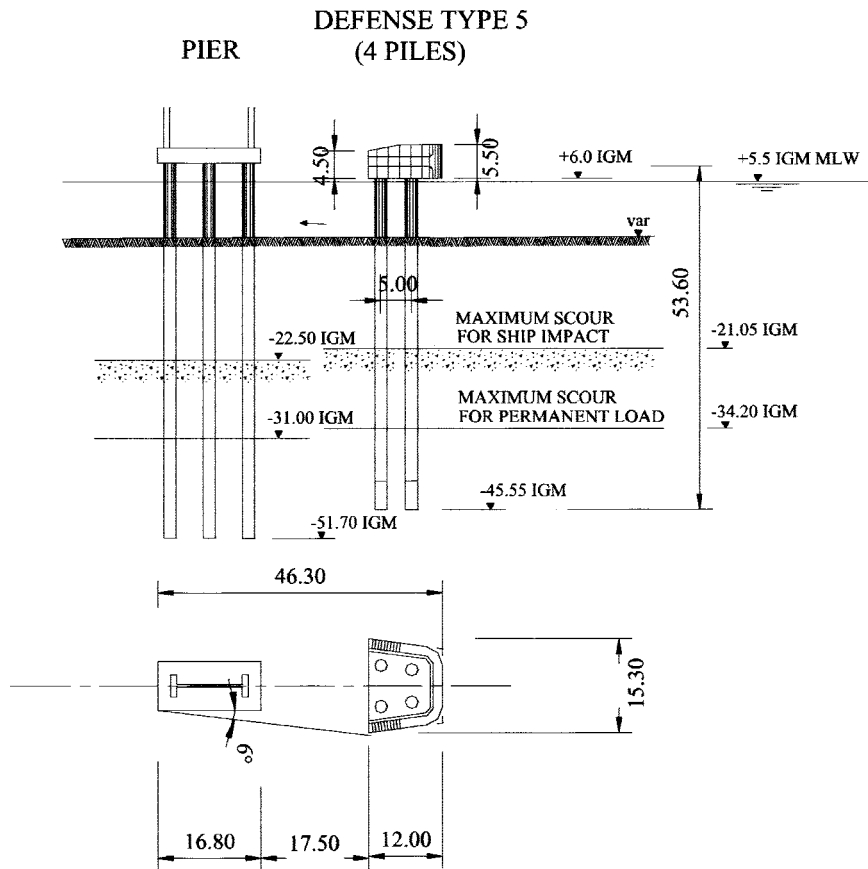


Fig. 3. Typical protection structure with four piles for piers of access viaduct

piles at the low design water level. The platforms have clear distances of 17.5 m to the bridge foundation to allow large horizontal displacements when subject to the design impact. The geometry and layout of the structure were developed to prevent the rake (overhang) of the design ship's bow from striking and causing damage to any portion of the bridge pier in case of a head-on collision.

The vertical piles are simply connected to the platform; i.e., they have no bending moment fixation in that joint. As a result of this feature, the piles are designed for bending without axial forces (pile tension and compression) due to impact, except for possible tension forces due to ship buoyancy if the rake is forced to displace downward as a consequence of the lateral displacements. The pile-cap connection was designed to transfer the horizontal impact force into the pile by shear. Each pile is designed to behave as a composite member made of an external structural steel tube filled with reinforced concrete. The pile casing is made of high strength steel with a yield strength of 690 MPa and a minimum tensile strength of 790 MPa, 24-mm thick in the areas of maximum bending moments. The pile lengths vary from approximately 55 to 60 m. The minimum pile spacing is 2.5 diameters (5.0 m) and the minimum number of piles per protection structure is four.

A defense structure for the pylon of the main bridge is shown in Fig. 2, and a typical defense structure for the piers of the access viaduct with four piles is shown in Fig. 3.

### Mechanical Behavior

The capacity to absorb the impact energy of the defense system originates with the load-deflection characteristics of the piles,

since the platform is very rigid and designed to enforce uniform displacements in all pile heads. The mechanical behavior of the piles under ship impact loads is a rather complex phenomenon due to the geometrically nonlinear behavior of the combined pile-soil system and the nonlinear mechanical properties of both the soil and the piles within the range of large expected deflections.

These structures must be capable of absorbing impact energy under various levels of scour, a situation that leads to difficulties in performing full-scale tests under real-life service conditions. The design of the defense structures and prediction of soil-pile behavior, must then rely on analyses by numerical models that have previously been calibrated by both appropriate laboratory tests and nonlinear analyses of the soil reaction.

A study of various possible scenarios showed that the condition of maximum scour requires the largest lateral displacement of the platform to absorb the design impact energy. The allowable lateral displacements of the pile top are limited by the maximum strains under tension of the casing steel at the plastic hinge. For maximum scour, displacements up to 15 m are reached, which resulted in the distance of 17.5 m of the protection structures to the bridge foundations, whereby an additional margin of clearance of 2.5 m is taken into account. These lateral displacements require that the equilibrium equations be formulated and solved for, accounting for the deformed configuration.

Special features of these structures are the large lateral displacement needed to absorb the design impact energy, which far exceeds those typical of most other structures. It is precisely this deformation capacity that allows the absorption of impact energy with reduced impact forces when compared with those generated by stiffer defense structures.

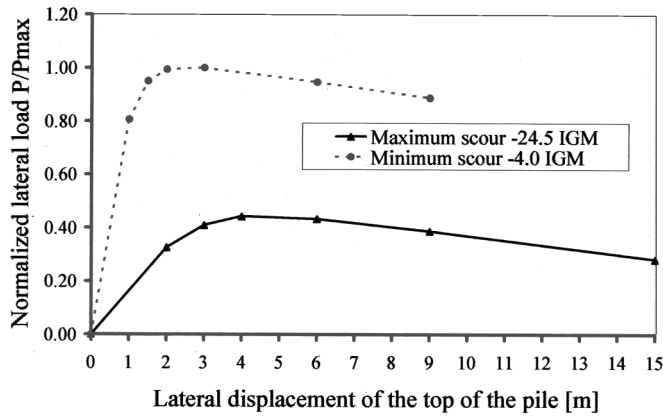


**Fig. 4.** Calculated structure response to lateral loads of single pile for two different scour conditions

The calculated structure response to lateral loads of any single pile of the structure of Fig. 3 is schematically shown in Fig. 4. The initial stiffness of the soil-pile,  $k_o$ , is controlled by the elastic properties of the pile shaft in bending and by the elastic restraint of the surrounding soil. While the soil parameters could easily be measured by performing full-scale small-amplitude dynamic tests of the piles, they do not control the maximum excursion of the top of the pile for the design impact.

In addition to the geometrically nonlinear terms for pile shafts, the mechanical response of the soil-pile system is influenced by the following phenomena:

- Inelastic response of the surrounding soil and pile-group effects.
- Concrete strains of about 5%, which are fifteen times larger than the maximum unconfined strain of concrete (about 0.35%).
- High compression strains in the steel casing, and potential for local buckling.
- Confinement of concrete by the steel casing and, reciprocally, lateral restraint of displacements of the steel casing by the encased concrete.
- Shear strength (cohesion and friction) of the interface between the concrete and the steel casing.

A particular feature of these piles is that the applied axial force is small as compared to its overall buckling load, which leads to a response controlled by bending. The bending load-deflection curve of a typical concrete-filled thin-walled steel tube increases monotonically until failure as shown by Prion and Boehme (1989). This curve presents a well-defined peak load at relatively small strains (0.4–1.0%) followed by a marked drop of load-bearing capacity for higher strains when subject to axial compression, as shown by O’Shea and Bridge (2000).

In relation to the mechanical behavior of concrete-filled steel pipes in bending, it is of particular interest to assess the effectiveness of the lateral outward support of the pipe-filling material and its influence on the buckling and postbuckling behavior of the steel casing. To gain insight in the nature of this process, preliminary reduced-scale laboratory tests were carried out as described below.

Two cylindrical 100 mm diameter pipes made of mild steel and 1.6 mm thickness, one filled with cement mortar and the other with graded dry sand, were tested in bending with the loading set up shown in Figs. 5(a and b). The transverse load was applied through a canvas bag filled with fine sand on approximately a quadrant of the pipe cross section and 300 mm axial length. The load was applied with the hydraulic system of the testing machine at a very low loading rate in order to improve control of the deformation process associated with buckling and postbuckling deformations.

The load-displacement curves of the tests are shown in Fig. 6. The concrete-filled tube (curve a) exhibited a monotonically increasing load until collapse; failure occurred by tension of the steel in the tension quadrant at the midspan section. The pipe wall presented a well-defined necking process and the localized tensile axial strains just before failure were measured to be approximately 30%. This result is in agreement with the strain observed in the tension test of a steel sample at the onset of necking. Simultaneously with the failure in tension, the tube developed an increase of the wavelike displacement in the compression side that had only been partially observed before failure because it was hidden under the loading pad. It was found that failure started at the tension side when the material reached its maximum axial stress in tension, and that the local buckling process on the com-

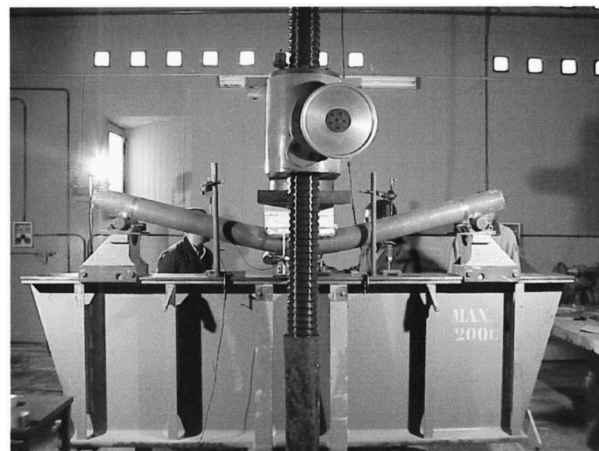
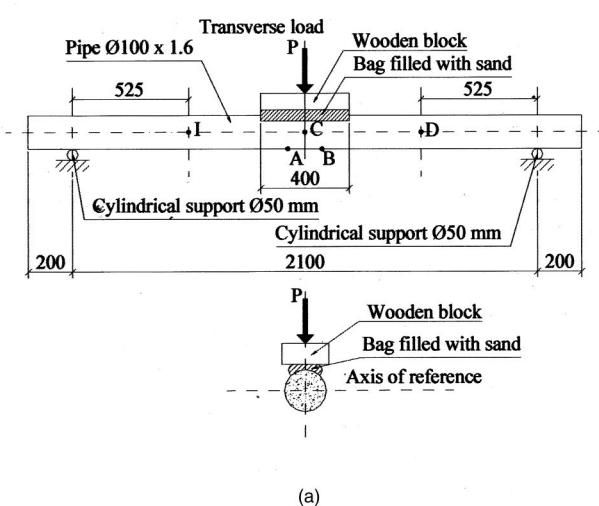


**Fig. 5.** (a) Laboratory test scheme; (b) Testing machine setup

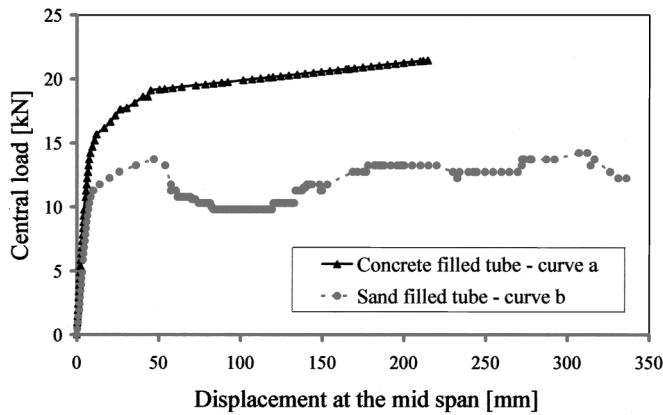


Fig. 6. Load-displacement curves of preliminary tests

pression side was not the direct cause of failure, but rather a consequence of it.

On the other hand, the test conducted on the sand-filled tube (curve b) exhibited several load peaks, each of them associated with the phases of the initial or of the postcritical buckling deformations. The test setup did not reach the collapse due to limitations of displacement of the loading device. Measurements of the plastic strains in tension made after the test confirmed that tension failure would have required additional deformations, and that the overall behavior was controlled by the postbuckling behavior of the compressed part of the cross section.

Another relevant aspect of the mechanical behavior of the concrete-filled tube in bending is related to the contribution of concrete to the load-carrying capacity of the tube for the large strains of the confined concrete, including the shear strength of the steel-concrete interface. It was observed that the confinement of concrete introduced by the steel pipe led to a significant contribution to the load-bearing capacity of the pile in bending, and that the tension failure of the pipe was caused by the longitudinal bending stresses rather than by the hoop stresses.

The nonlinear mechanical properties of the confined concrete at large strains, the shear capacity of the concrete-steel interface, and the lateral restraint given by concrete to the steel were taken into account by using reduced-scale models according to the similitude laws. These issues could also be addressed through analysis by means of a nonlinear 3D finite-element analysis program. However, the need to assess by testing the various parameters of the numerical model of the composite structure led to use of reduced-scale models to calibrate the simpler numerical analyses based on nonlinear beam theory.

### Reduced Scale Laboratory Tests

The nonlinear response of a typical pile shaft was investigated by means of reduced-scale models tested in the laboratory with the same layout shown in Figs. 5(a and b). The geometrical scale of the models was 1:15; the concrete mix used for the model was designed so as to have the same strength and stiffness of the concrete used in the full-scale piles, with a characteristic compressive strength of 34 MPa. The casing of the models was fabricated with steel of 360 MPa mean yield stress and a mean tensile strength of approximately 590 MPa. These properties were chosen so that the stress scale of the models was as close as possible to 1:1 with the steel sheets available in the market, taking

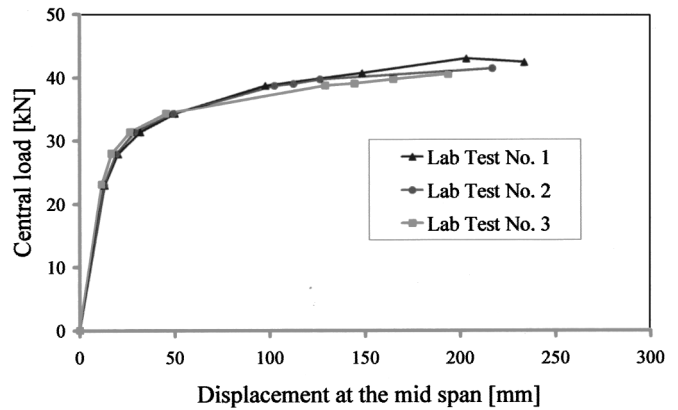


Fig. 7. Load-displacement curves of reduced-scale laboratory tests

into account that the steel to be used in the fabrication of the full-scale tubes had a specified yield stress of 690 MPa and strength of 790 MPa. This was adopted in order to represent the mechanical behavior of the piles, including their nonlinear response and buckling. The transverse load was applied with a loading pad of 400 mm length along the axis of the model.

The load deflection curves are given in Fig. 7. They show a continuously increasing load with the transverse displacement up to the failure in tension at midspan. The incipient buckling waves on the compression side at midspan are shown in Fig. 8(a), and the radius of curvature of the residual plastic deformation of the specimens is given in Table 1.

The neutral axis of all tested specimens, as defined through the deformations of the grid, was found above the center of the cross section. This suggests that the concrete contributes to the stiffness and strength of the shaft in bending up to failure, even though the concrete strains are more than twenty times larger than the unconfined compression breaking strain of concrete.

In order to verify whether the length of the loading pad had any influence on the mechanical behavior of the models, the third model was tested subject to two symmetrical concentrated loads 200 mm apart. No appreciable difference with respect to the models tested with distributed loads was found in either the failure load or the load-deflection curve. This was considered an additional indication that local buckling of the compression zone did not have any significant influence on the failure mechanism, and that failure occurred due to tension failure of the steel.

### Numerical Model

The analysis of the pile-soil system of the protection structures was carried out by means of a numerical model with the software program SOFISTIK based on a nonlinear formulation of beam elements and of nonlinear lateral springs. The basic assumptions were:

- The beam elements are prismatic and have no shear deformations.
- The beam element represents a composite member made of an external steel tube filled with concrete. Steel and concrete are assumed to have no relative displacement at their contact surfaces. The stress-strain curve of steel is that obtained from simple tensile tests. The stress-strain of concrete are those obtained from simple compression tests. The volume of concrete subject to longitudinal tensile stresses is not accounted for.

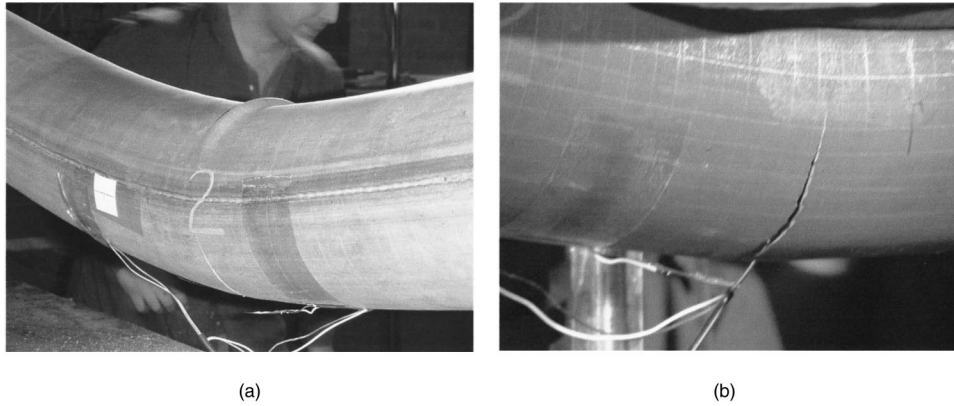


**Fig. 8.** (a) Incipient buckling waves on compression side at midspan; (b) Failure of filled tube in tension at midspan

- The linearized equilibrium equations are formulated in the deformed configuration with second order theory.
- The nonlinear properties of the soil together with the pile-group effect strongly influence the response of the pile-soil system. The soil reaction springs have bilinear material properties, from initial elastic values to a perfectly plastic condition. These parameters, including the pile group effects, were obtained from an analysis with the software program PLAXIS, whereby the soil had been analyzed by means of 2D finite-element models of different horizontal layers of soil including the pile cross sections as rigid inclusions.

To assess the model for the nonlinear behavior of the composite beam elements with large strains and rotations, a test calculation was conducted to simulate the laboratory tests. The stress-strain relation for the steel was represented by both bilinear and trilinear curves adjusted to the results of three simple tensile tests of steel samples [Figs. 9(a and b)]. Stress-strain characteristics of concrete were modeled with the standard uniaxial stress-strain relationship for a mean compressive strength of 34 MPa up to an axial strain of 10%, followed by a segment of perfectly plastic material (without degradation) for strains larger than 10% up to failure [Fig. 9(c)]. Results of the numerical model and of the laboratory tests are compared in Fig. 10.

The calculated load-deflection curves turn out to be close but somewhat lower than those of the tests, thus confirming the validity of the basic assumptions of the numerical model on the mechanical behavior of the composite pile.

As was mentioned earlier in this paper, the nonlinear characteristics of the soil in contact with the pile shaft cannot be verified by direct measurements, due to the variable scour conditions for which the defense system has to be designed. In addition to the problem of identifying the nonlinear mechanical properties of the soil layers under the real design conditions of confinement, the construction procedure may lead to an alteration of the soil in the contact area with the piles that can only be estimated at design

**Table 1.** Radius of Curvature at Failure Cross Section of Filled Tube Test in Laboratory

Tube	Radius of curvature (m)
1.1	0.91
2.1	0.97
3.1	1.12

stage. For these reasons, the designer performed a sensitivity analysis of the influence of variations of the soil spring values that may be expected to occur as a consequence of the actual field conditions.

A typical computed load-deflection curve of the top of the pile under an increasing horizontal load applied to that point of the structure is shown in Fig. 4 for two different scour conditions and in Fig. 11 for two sets of (maximum and minimum) soil parameters. As expected, the largest displacements at the top are associated with the combination of maximum scour and lower limits of the soil parameters. Although direct assessment of the soil spring parameters does not appear practicable within the time frame of the design and independent review of these structures, an indirect approach was chosen whereby the load deflection characteristics of 1:15 scale models of the piles were performed at the site. These additional tests are discussed next.

### Reduced-Scale Field Tests

While the reduced-scale model tests performed in the laboratory provided useful information to assess the mechanical assumptions of the steel composite piles in bending, several assumptions adopted for the purpose of design and analysis were still left lacking direct confirmation due to shortcomings of the tests. The main limitations of the tests were:

- The bending moment diagram and support conditions of the tests differ in comparison with those existing in the field,
- The location of the maximum bending moment section in the lab tests is predetermined, while that in the field is a consequence of the distribution of soil reactions, and
- The loading pad used to apply the transverse load in the lab tests does not accurately represent the nonlinear lateral reaction of the actual soil in the field.

To improve on these limitations, additional reduced-scale tests were carried out in the field according to the layout shown in Fig. 12(a). The pile models [Fig. 12(b)] were embedded on fine sand extracted from the river as hydraulic fill, and the load was applied through a taut cable instrumented with a load cell. The main purpose of these additional tests was to find out if the soil-pile interface typical of the embedded piles had any appreciable influence on the ultimate bending moment and maximum curvature that could be developed in conditions closer to those of the full-scale piles.

An important limitation to representing the passive soil resistance with a reduced-scale model is imposed by the confinement

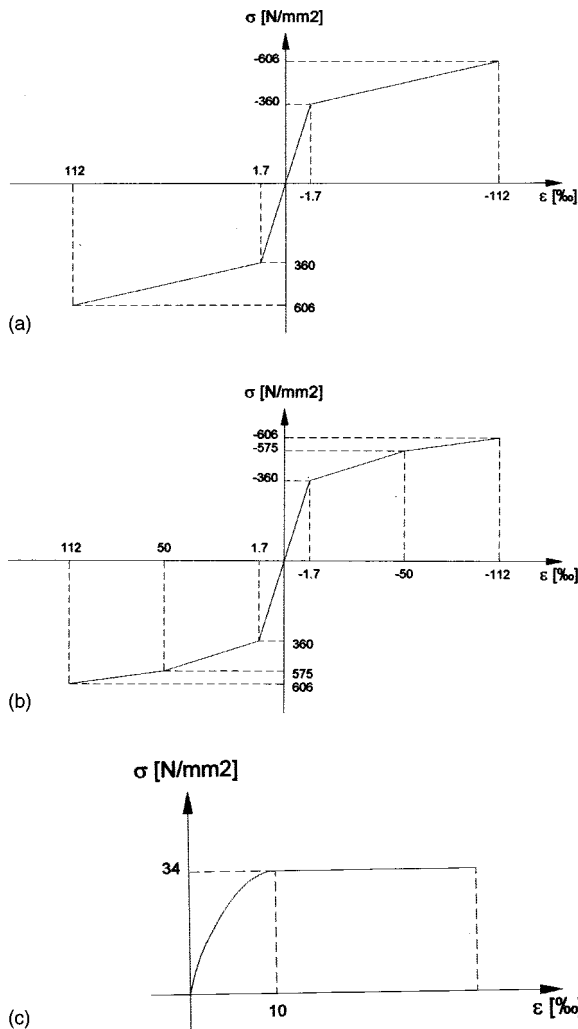


Fig. 9. (a) Bilinear stress-strain curve of tube steel; (b) Trilinear stress-strain curve of tube steel; (c) Stress-strain curve of concrete

stresses in the soil. Since the geometrical scale of the model is 1:15 and the stress scale is 1:1, the effective confinement pressure due to the soil overburden cannot be reproduced in the model unless the soil model has a density 15 times larger than that of the real soil. Since the soil of the model is the same as the full-scale structure, the law of similitude between model and full-scale is not satisfied. As an approximation, however, it is possible to improve the confinement pressure of the reduced-scale models by applying vertical prestressing to the soil of the model to reproduce the real confinement.

The prestressing was chosen to simulate the effective confinement pressure of the soil at the depth where the numerical model gave the maximum bending moment on the pile. This was achieved by means of three posttensioned strands anchored in reaction blocks buried at the depth of the pile tip; two of these tendons were applied on the loading side and one on the opposite side.

The piles were instrumented with electrical resistance strain gauges at three different sections in order to estimate the location of the maximum bending moment as the horizontal load was increased. These sections were located as follows: one at the soil grade, and two in sections 0.25 and 0.50 m below. From the strain measurements obtained in these tests for all loads levels, it was found that the maximum bending moment took place approxi-

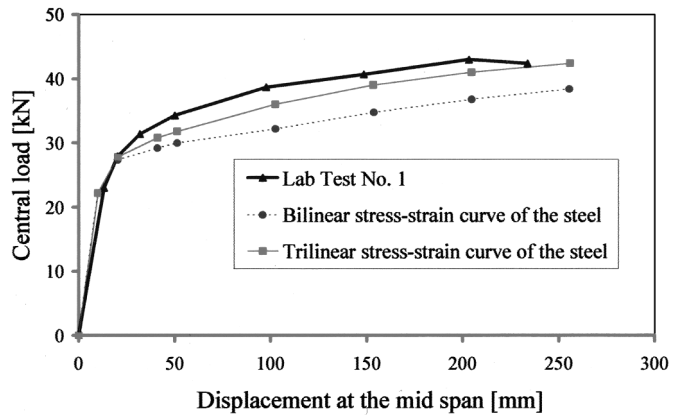


Fig. 10. Results of numerical model and laboratory tests

mately two pile diameters below soil grade. For test number 1 the soil prestressing was applied as described above, while for test numbers 2 and 3, the prestressing forces were 50% of those of test number 1.

The load-deflection curves from these tests are shown in Fig. 13, and the maximum residual curvature of test number 1 is shown in Fig. 14. It is pointed out that the load-deflection curves of Fig. 13 exhibit an inflexion point due to geometrical nonlinearities derived from the rotations of both the structure and the applied lateral load. This is not the case in the lab tests, where the applied load and the reactions did not change direction during the tests. This effect can be corrected by calculating the bending moment taking into account these rotations and using the bending moment as the controlling variable rather than the external force.

For test number 1, which represents more closely the expected soil conditions of the full-scale piles, the applied horizontal force associated with a deflection of 1 m was equal to 10.6 kN and a corresponding bending moment of 21 kNm.

Fig. 15 presents a comparison of the load-displacement curve of number 1 with that obtained with a numerical model of the test. The load-displacement curve for the soil springs was taken as bilinear (elasto-perfectly plastic). All springs in the top 0.7 m of soil were calculated assuming the same elastic modulus of 47.5 MPa, which corresponds to the expected modulus of the soil at a depth of two pile diameters below grade (4 m) in the full-scale pile. The passive soil pressure was also assumed constant in the

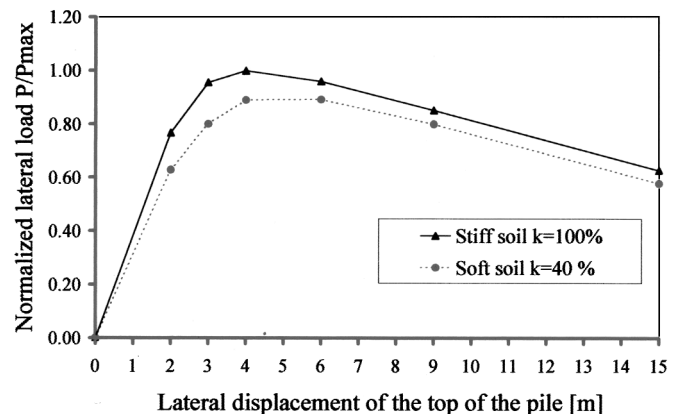
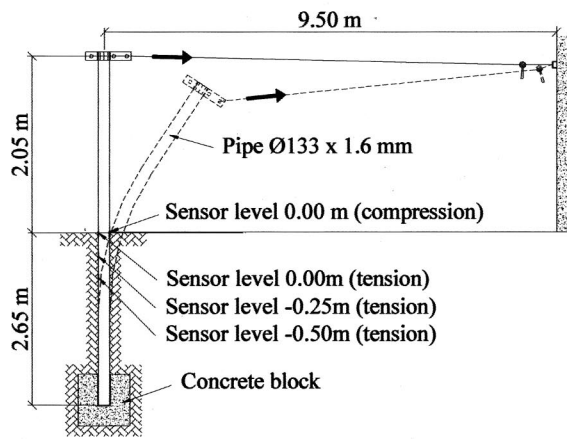
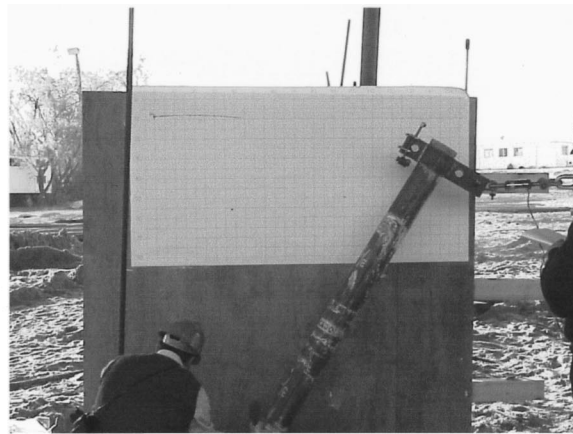


Fig. 11. Calculated structure response to lateral loads of single pile for two sets of soil parameters



(a)



(b)

Fig. 12. (a) Layout of reduced-scale field tests; (b) Reduced-scale field test of filled tube

top 0.70 m with  $K_p = 4$  and a constant effective overburden pressure of  $40 \text{ kN/m}^2$ . These values are consistent with the vertical prestressing of  $40 \text{ kN/m}^2$  applied for test number 1. For depths larger than 0.70 m, the passive strength of the soil was taken as four times that of the top layers to account for the concrete blocks built at the tip of the pile.

Since the numerical model accounts only up to second-order effects, the value of the load from the tests was modified to produce the same bending moments of the test, taking into account the large displacements and rotations involved. The results of the numerical model follow closely the model tests except for very large displacements (larger than 1 m in the horizontal direction). The larger stiffness observed in the tests, not reflected in the numerical results, may be attributed to an increase of the passive soil resistance when the angle of rotation of the pile shaft becomes sufficiently large as to deviate from the horizontal passive resistance assumed in the calculations.

The bending moment of the full-scale pile predicted from the test results can be obtained by multiplying the bending moment of the model ( $0.021 \text{ MNm}$ ) by the following factors: force scale (225), geometrical scale (15), and strength factor equal to the ratio of the tensile strength of the steel of the full-scale pile to that of the model ( $790/590 = 1.32$ ). This leads to an ultimate bending

moment prediction of  $94.9 \text{ MNm}$ , which is in acceptable agreement with the design value of  $89.3 \text{ MNm}$  given by the numerical model.

The load-deflection curves of test numbers 2 and 3 indicate that the lateral displacements are considerably larger when the soil stiffness is reduced. However, the most important result is that the energy dissipation is only marginally smaller than for the expected soil stiffness. The field model tests also showed that the maximum curvature that can be developed in the field with a more realistic distribution of the reaction transmitted by the soil to the pile is comparable to that obtained in the lab tests.

## Conclusions

The results of the numerical analyses performed for design of the piles have been shown in acceptable agreement with those resulting from laboratory and field tests of reduced-scale models. These tests showed that numerical analysis based on the assumption that the concrete remains effective in transmitting shear and compression stresses up to failure is valid in predicting the energy dissipation capacity of the piles. In fact, special connectors adopted in

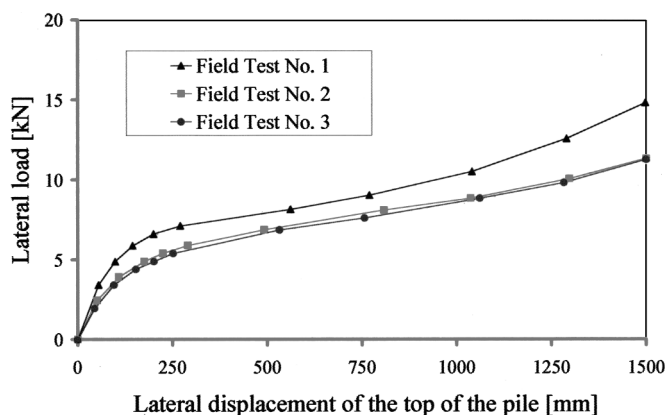


Fig. 13. Load-displacement curves from reduced-scale field tests

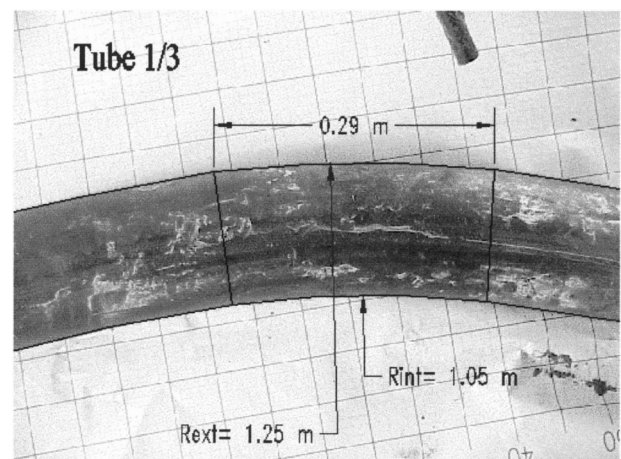
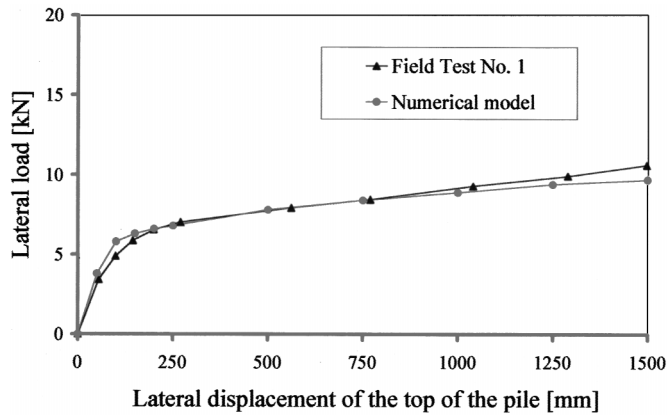


Fig. 14. Minimum radius of residual curvature



**Fig. 15.** Comparison of numerical analysis versus reduced-scale field test

the design to enhance the shear strength of the steel-concrete interface provide an extra margin of safety against local outward buckling displacements of the steel casing, added to that already confirmed by the present tests of models without such connectors.

Both laboratory and field tests of the reduced-scale models confirmed that concrete inside the piles contributes to the load-carrying capacity in bending even for very large deformations,

and that the piles fail when maximum stresses in the steel casing reach its tensile strength.

## References

- American Association of State Highway and Transportation Officials (AASHTO). (1991). *AASHTO guide specification and commentary for vessel collision design of highway bridges, Vol. I: Final report*, Washington, D.C.
- O'Shea, M., Bridge, R., (2000). "Design of circular thin-walled concrete filled steel tubes." *J. Struct. Eng.* 126(11), 1295–1303.
- Prion, H. G. L., and Boehme, J. (1989). "Beam-column behavior of steel tubes filled with high strength concrete." *Proc., 4th Int. Colloquium, North American Session*, Structural Stability Research Council, New York, 439–450.
- Saul, R., and Svensson, H. (1982). "On the theory of ship collision against bridge piers." *IABSE Proc. P-51*, International Association of Bridge and Structural Engineers, Zurich, 29–38.
- Saul, R., and Svensson, H. (1983). "Means of reducing the consequences of ship collisions with bridges and offshore structures." *Proc., IABSE Int. Colloquium on Ship Collision with Bridges and Offshore Structures*, International Association of Bridge and Structural Engineers, Zurich, 165–179.
- Saul, R., Humpf, K., and Patsch, A. (2001). "The Rosario-Victoria cable-stayed bridge across the river Paraná in Argentina and its ship impact protection system." *Proc., Int. Conf. on Steel and Composite Structures*, Pushan, Korea.
- Terndrup Pedersen, P. et al., (1993). "Ship impacts: bow collisions." *Int. J. Impact Eng.* 13(2), 163–187.